

The electromagnetic field effects in in-out and in-in formalisms

Gaoqing Cao

School of Physics and Astronomy, Sun Yat-sen University, Guangzhou 510275, China.

(Dated: May 14, 2020)

In this work, we compare the effects of electromagnetic (EM) fields on strong coupling systems in two formalisms: in-out and in-in, which are different from each other when a finite electric field is present. The chiral effective Nambu–Jona-Lasinio model is adopted for this study, and two kinds of EM field distributions are considered: pure electric field and parallel EM (PEM) field with equal electric and magnetic components. For both distributions, we find that the results of in-out and in-in formalisms start to diverge when the electric field $(qE)^{1/2}$ is larger than the chiral effective mass $M = [m^2 + (\pi^0)^2]^{1/2}$, that is, when the Schwinger pair production mechanism becomes important. Besides, the chiral restorations are stiffer in the in-in formalism, especially the transition shifts to first-order instead of the second-order for the PEM field. The neutral collective modes are also explored accordingly: For the PEM field, more precise calculations show nonmonotonic features of their pole masses due to parity mixing, and then the Goldstone-like mode is found to be noneffective at the end of chiral rotation because of chiral anomaly.

I. INTRODUCTION

In peripheral heavy ion collisions, the strongest electric (E) and magnetic (B) fields of recent Universe were expected to be produced in the fireball [1–4], due to the short distance between heavy ions and large Lorentz factors for their relativistic motions, respectively. The magnitude of the magnetic field is $10^{18} - 10^{20}$ Gauss or $(0.1 - 1 \text{ GeV})^2$ in natural unit, which is comparable to the energy scale of QCD: $\Lambda_{\text{QCD}} \sim 0.2 \text{ GeV}$ thus would have a non-negligible effect on the ground state. By following such philosophy, numerical simulations were carried out in the first-principle lattice QCD which wouldn't suffer from *sign problem* for finite B . While confirming the sophisticated *magnetic catalysis effect* at low temperature [5, 6], they also discovered an unexpected feature of QCD around the pseudo-critical temperature, the so called "*inverse magnetic catalysis effect*" [7, 8]. There are several proposals for this puzzle [9–16] but it remains an open question. Associated with the shift of ground state, the dispersions of either the neutral or charged collective modes (mesons) will change accordingly. For example, the pole mass responds as the following [17–24]: it decreases for neutral pion and charged rho mesons but increases for charged pions with not too strong magnetic field.

At large enough temperature when chiral symmetry is approximately restored [25, 26], macroscopic chiral anomaly phenomena [27–33] can emerge to an observable level, which is now a very important scientific target of the phase II program of Beam Energy Scan in STAR [34–36]. Among all the circumstances for anomaly, the one with parallel electromagnetic (PEM) field is specific because the background is already parity-violating even without involving any matter. In our previous studies [37, 38], neutral pseudo-scalar mesons were found to condensate under the PEM field; and P. Copinger and K. Fukushima discovered that the Schwinger pair production (SPP) rate is enhanced by a semilocalized static magnetic field [39]. Furthermore, there is one very im-

portant discovery for the chiral anomaly dynamics [40]: In order to understand the contradiction between massless case and small mass limit for chiral anomaly $\partial_\mu J_5^\mu$, one has to adopt the in-in (or real-time) rather than the in-out (or imaginary-time) propagator for the fermions. The in-out propagator was derived by Schwinger in 1951 under the proper-time formalism, while the in-in propagator was obtained by solving the real-time Dirac equation directly. The advantage of the in-in propagator is that it captures the right SPP rate in the presence of electric field, see the detailed discussions in Ref. [41]. Physically, the main difference between in-in and in-out schemes is whether the feedback of SPP has been taken into account or not in electric field [42]. So we can identify the *unobserved yet* Schwinger mechanism indirectly by comparing the mesonic properties detected in heavy ion collisions with those predicted in these formalisms.

It constitutes the main motivation of our recent work to compare the "order parameters" of chiral symmetry and the associated collective modes in both in-out and in-in formalisms. This would give some indications on the validity of the much simpler and more commonly used in-out formalism for the study of electric field effect. The paper is arranged as follows: In Sec. II, we derive the "gap equations" universally for both in-out and in-in formalisms, which are then regularized in a "vacuum regularization" like scheme. Sec. III is devoted to the analytical calculations and regularizations of the polarization functions in the in-in formalism. We illuminate our numerical results for pure electric field and PEM field in Sec. IV and pay special attention to the instability at the end of chiral rotation. A simple summary is given in Sec. V.

II. "GAP EQUATIONS" IN PARALLEL ELECTROMAGNETIC FIELD

For simplicity and without loss of generality, we adopt one-flavor Nambu–Jona-Lasinio (NJL) model for the

study of strong coupling systems in the presence of parallel electromagnetic field. The Lagrangian density is given by the following form [26, 43, 44]:

$$\mathcal{L}_{\text{NJL}} = \bar{\psi}(i\not{D} - m_0)\psi + G[(\bar{\psi}\psi)^2 + (\bar{\psi}i\gamma^5\psi)^2], \quad (1)$$

where the spinor ψ represents the u quark field, m_0 is the current quark mass, and G is the four-fermion coupling constant. The PEM field is introduced through the covariant derivative $D_\mu = \partial_\mu + iqA_\mu$ with the vector potential chosen explicitly as $A_\mu = (iEz, 0, -Bx, 0)$ and the u quark charge $q = 2/3e$. The signs of E and B are not so important for our study, thus we stick to the case with $E, B \geq 0$. For small m_0 , the Lagrangian has approximate $U_L(1) \otimes U_R(1)$ chiral symmetry.

In in-out time formalism (IOF), the system is assumed to be in equilibrium and the ground state can be explored by following the standard procedure [37, 38]. We introduce two auxiliary neutral boson fields via the Hubbard-Stratonovich transformation: $\sigma(x) = -2G\bar{\psi}(x)\psi(x)$ and $\pi^0(x) = -2G\bar{\psi}(x)i\gamma^5\psi(x)$, then the action can be bosonized by integrating out the quark degrees of freedom as:

$$\mathcal{S}_{\text{NJL}} = \int d^4x \frac{\sigma^2 + (\pi^0)^2}{4G} - \text{Tr} \ln [i\not{D} - m_0 - \sigma - i\gamma^5\pi^0] \quad (2)$$

In recent work, we only consider homogeneous chiral condensates with the expectation values: $\langle\sigma(x)\rangle \equiv m - m_0$ and $\langle\pi^0(x)\rangle \equiv \pi^0$. Then the gap equations can be obtained by minimizing the thermodynamic potential $\Omega \equiv \mathcal{S}_{\text{NJL}}/V_4$ with respect to these order parameters, that is, $\partial\Omega/\partial x = 0$ ($x = m, \pi^0$), as:

$$\frac{m - m_0}{2G} - \frac{1}{V_4} \text{Tr} \mathcal{S}(x, x') = 0, \quad (3)$$

$$\frac{\pi^0}{2G} - \frac{1}{V_4} \text{Tr} \mathcal{S}(x, x')i\gamma^5 = 0. \quad (4)$$

Here, $\mathcal{S}(x, x') \equiv -[i\not{D} - m_0 - \sigma - i\gamma^5\pi^0]_{xx'}^{-1}$ is the operator form of quark propagator, V_4 is the four dimensional space-time volume in Euclidean space, and the trace should be taken over the coordinate, Dirac and color spaces.

Expand the action Eq.(2) to quadratic orders of the fluctuation fields: $\hat{\sigma}(x) \equiv \sigma(x) - \langle\sigma\rangle$ and $\hat{\pi}^0(x) \equiv \pi^0(x) - \langle\pi^0\rangle$ and transform to energy momentum space, the polarization functions can be generally written in the random-phase approximation (RPA) as

$$\Pi_{\text{MM}'}(q) = \int \frac{d^4p}{(2\pi)^4} \text{Tr} \hat{S}(q+p)\Gamma_M\hat{S}(p)\Gamma_{M'} \quad (5)$$

with the interaction vertices given by

$$\Gamma_{\hat{\sigma}} = 1, \quad \Gamma_{\hat{\pi}^0} = i\gamma^5. \quad (6)$$

In the matrix form, the polarization function can be represented in the parity-doublet space as:

$$\Pi(q) = \begin{pmatrix} \Pi_{\hat{\sigma}\hat{\sigma}}(q) & \Pi_{\hat{\sigma}\hat{\pi}^0}(q) \\ \Pi_{\hat{\pi}^0\hat{\sigma}}(q) & \Pi_{\hat{\pi}^0\hat{\pi}^0}(q) \end{pmatrix}. \quad (7)$$

Then, the matrix form of the inverse of the effective mesonic propagator follows directly:

$$\mathcal{G}^{-1}(q) = \frac{1}{2G} + \Pi(q). \quad (8)$$

By diagonalizing \mathcal{G}^{-1} , we obtain the inverse propagators of the mass eigen modes, which we denote by "Σ" and "Π⁰", as:

$$\mathcal{G}_{\Sigma}^{-1} = \frac{1}{2} \left[\frac{1}{G} + \Pi_{\hat{\sigma}+\hat{\pi}^0} + \sqrt{(\Pi_{\hat{\sigma}-\hat{\pi}^0})^2 + 4(\Pi_{\hat{\sigma}\hat{\pi}^0})^2} \right],$$

$$\mathcal{G}_{\Pi^0}^{-1} = \frac{1}{2} \left[\frac{1}{G} + \Pi_{\hat{\sigma}+\hat{\pi}^0} - \sqrt{(\Pi_{\hat{\sigma}-\hat{\pi}^0})^2 + 4(\Pi_{\hat{\sigma}\hat{\pi}^0})^2} \right] \quad (9)$$

with $\Pi_{\hat{\sigma}\pm\hat{\pi}^0} \equiv \Pi_{\hat{\sigma}\hat{\sigma}} \pm \Pi_{\hat{\pi}^0\hat{\pi}^0}$.

In in-in formalism (IIF), the forms of the "gap equations" would remain the same as Eqs.(3) and (4) by following the definitions of the auxiliary boson fields or the Hartree approximation. But there is no self-consistent thermodynamic potential for these "gap equations" when the feedback of Schwinger mechanism is included explicitly, see discussions later. Nevertheless, we can still use RPA to explore the effective collective excitations in IIF by following the same chain diagrams as in IOF [26]. Eventually, the pole masses of the collective modes can be evaluated by setting $\mathcal{G}_{\text{M}}^{-1}(q_4 = im_{\text{M}}, \mathbf{q} = 0) = 0$ in IOF and $\mathcal{G}_{\text{M}}^{-1}(q_0 = m_{\text{M}}, \mathbf{q} = 0) = 0$ in IIF with $\text{M} = \Sigma, \Pi^0$.

Now, the difference between IOF and IIF just originates from the different forms of quark propagator adopted in the calculations. The explicit form of the propagators and the consequential derivations have already been given in Ref. [38] for IOF, so we mainly focus on carrying out analytic derivations under the IIF in the following. In IIF, the quark propagator can be written out explicitly in coordinate space as $\mathcal{S}(x, x') = \Phi(A)\tilde{S}(x - x')$ with the Schwinger phase $\Phi(A) \equiv e^{-iq \int_{x'}^x A_\mu dx^\mu}$ and the effective propagator [40]

$$\begin{aligned} \tilde{\mathcal{S}}(y) = & \frac{-i q B q E}{(4\pi)^2} \int_{RT} ds \exp \left\{ -i M^2 s + \frac{i}{4} \left[\frac{q B}{\tan(q B s)} (y_1^2 + y_2^2) + \frac{q E}{\tanh(q E s)} (y_3^2 - y_0^2) \right] \right\} \\ & \left\{ m - i \gamma^5 \pi^0 - \frac{q B}{2} \left[(\cot(q B s) \gamma^1 + \gamma^2) y_1 + (\cot(q B s) \gamma^2 - \gamma^1) y_2 \right] - \frac{q E}{2} \left[(\coth(q E s) \gamma^3 - i \gamma^4) y_3 \right. \right. \\ & \left. \left. + (\coth(q E s) \gamma^4 + i \gamma^3) i y_0 \right] \right\} \left[\cot(q B s) \coth(q E s) + i \gamma^5 + \coth(q E s) \gamma^1 \gamma^2 + i \cot(q B s) \gamma^4 \gamma^3 \right]. \end{aligned} \quad (10)$$

Here, we've defined variables $y \equiv x - x'$, $M^2 \equiv m^2 + (\pi^0)^2$ and the RT integral path

$$\int_{RT} \equiv \left(\int_{-\infty - i S_E}^{-i S_E - \epsilon} + \int_{\infty - i S_E/2}^{-\infty - i S_E/2} + \int_0^{-\infty} \right) \theta(y_3) + \left(\int_{\infty - i S_E}^{-i S_E + \epsilon} + \int_0^{\infty} \right) \theta(-y_3) \quad (11)$$

with the SPP parameter $S_E = \pi/|qE|$. In principle, there should be delta function terms that are from the derivatives $\partial_{x_3} \theta(\pm y_3)$ in the effective propagator Eq. (10) [40]. But we neglect them as their total contribution is infinitesimally small in energy momentum space thus not relevant to our recent study, similar to the discussions in Eq. (12) and below. At this point, the only difference between the in-out and in-in propagators is the additional integral branches in IIF, that is, the S_E dependent terms on the right-hand side of Eq.(11) which account for the feedback of SPP.

Take the first branch of the path for $y_3 > 0$ for example and keep only the m and y_3 relevant terms, we can use the following representation of θ function

$$\theta(y_3) = \frac{1}{2\pi i} \int_{-\infty}^{\infty} dq_3 \frac{e^{i q_3 y_3}}{q_3 - i \eta}, \quad \eta \rightarrow 0^+$$

to carry out Fourier transformation and find:

$$\begin{aligned} & \frac{1}{2\pi i} \lim_{\eta \rightarrow 0^+} \int dy_3 e^{-i p_3 y_3} \int_{-\infty}^{\infty} dq_3 \frac{e^{i q_3 y_3}}{q_3 - i \eta} \int_{-\infty - i S_E}^{-i S_E - \epsilon} ds e^{\frac{i}{4} \frac{q E}{\tanh(q E s)} y_3^2} \left[m - \frac{q E}{2} (\coth(q E s) \gamma^3 - i \gamma^4) y_3 \right] \\ &= \frac{1}{2\pi i} \lim_{\eta \rightarrow 0^+} \int_{-\infty}^{\infty} dq_3 \frac{1}{q_3 - i \eta} \int_{-\infty}^{-\epsilon} ds e^{-i \frac{\tanh(q E s)}{q E} (p_3 - q_3)^2} \left(\frac{-i}{4\pi \tanh(q E s)} \frac{q E}{\tanh(q E s)} \right)^{-\frac{1}{2}} \left[m - (\gamma^3 - i \tanh(q E s) \gamma^4) (p_3 - q_3) \right] \\ &= \int_{-\infty}^{-\epsilon} ds \left[(m - (\gamma^3 - i \tanh(q E s) \gamma^4) p_3) G \left(p_3, \frac{\tanh(q E s)}{q E} \right) \left(\frac{-i}{4\pi \tanh(q E s)} \frac{q E}{\tanh(q E s)} \right)^{-\frac{1}{2}} - i (\gamma^3 - i \tanh(q E s) \gamma^4) \right], \end{aligned} \quad (12)$$

where the auxiliary function is

$$G(p_3, x) = \frac{e^{i p_3^2 x}}{2} \left[1 - (1 + i) C \left(\sqrt{\frac{2x}{\pi}} p_3 \right) - (1 - i) S \left(\sqrt{\frac{2x}{\pi}} p_3 \right) \right]$$

with $C(x)$ and $S(x)$ the Fresnel integrals. The contribution of the integral path $s = -i S_E + \epsilon e^{i\theta}$ with $\theta \in [\pi, \pi/2]$ is infinitesimally small over the integrand of Eq.(12) thus can be neglected for the Fourier transformation. Similar argument applies to the integral path $\int_{-i(S_E - \epsilon)}^{-i S_E + \epsilon} \theta(-y_3)$. Finally, the path \int_{RT} can be simply represented as

$$\int_{\Gamma_\epsilon} \equiv \int_0^{\infty} - \int_{-i(S_E - \epsilon)}^{\infty - i(S_E - \epsilon)}$$

for the quark propagator in energy momentum space, as no singularity is encountered during the deformation of the integral path for $y_3 > 0$. The aforementioned delta function terms are similar to the last term in the square bracket of Eq.(12), thus cancel out due to the fact that $\partial_{x_3} \theta(y) = -\partial_{x_3} \theta(-y)$ and the continuity of the integrand around $s = -i S_E$. Now, it is straightforward to take full Fourier transformation of the effective propagator Eq. (10) to get

$$\begin{aligned} \hat{\mathcal{S}}(p) = & i \int_{\Gamma_\epsilon} ds \exp \left\{ -i(M^2 - i\eta)s - i \frac{\tan(q B s)}{q B} (p_1^2 + p_2^2) - i \frac{\tanh(q E s)}{q E} (-p_0^2 + p_3^2) \right\} \\ & \left[m - i \gamma^5 \pi^0 + i \gamma^4 (p_0 + \tanh(q E s) p_3) - \gamma^3 (p_3 + \tanh(q E s) p_0) - \gamma^2 (p_2 + \tan(q B s) p_1) \right. \\ & \left. - \gamma^1 (p_1 - \tan(q B s) p_2) \right] \left[1 + i \gamma^5 \tanh(q E s) \tan(q B s) + \gamma^1 \gamma^2 \tan(q B s) - i \gamma^4 \gamma^3 \tanh(q E s) \right], \end{aligned} \quad (13)$$

the integrand of which is the same as that in IOF [38].

As the delta functions in the quark propagator do not play roles in the evaluations of the order parameters, the traces over the propagator can be carried out explicitly to obtain

$$\frac{1}{V_4} \text{Tr } \mathcal{S}(x, x) = N_c m K(M, E, B) - N_c \frac{\pi^0 q E q B}{4\pi^2 M^2} \left(1 - e^{-M^2 S_E}\right), \quad (14)$$

$$\frac{1}{V_4} \text{Tr } \mathcal{S}(x, x) i\gamma^5 = N_c \pi^0 K(M, E, B) + N_c \frac{m q E q B}{4\pi^2 M^2} \left(1 - e^{-M^2 S_E}\right), \quad (15)$$

$$K(M, E, B) = \Re \left\{ \int_0^\infty \frac{ds}{4\pi^2} e^{-M^2 s} \left[\frac{qB}{\tanh(qBs)} \frac{qE}{\tan(qEs)} - e^{-M^2 S_E} \frac{qB}{\tanh(qB(s + S_E))} \frac{qE}{\tan(qEs)} \right] \right\}, \quad (16)$$

where we can easily identify the feedback of SPP from the terms with $e^{-M^2 S_E}$. Similar to the "vacuum regularization" scheme, we introduce subtract terms that make sure the convergence of the proper-time integral and then are presented by three-momentum cutoff, that is,

$$K^r(M, E, B) = \Re \left\{ \int_0^\infty \frac{ds}{4\pi^2} e^{-M^2 s} \left[\frac{qB}{\tanh(qBs)} \frac{qE}{\tan(qEs)} - \frac{1}{s^2} - e^{-M^2 S_E} \left(\frac{qB}{\tanh(qB(s + S_E))} \frac{qE}{\tan(qEs)} - \frac{1}{s(s + \tilde{S}_E(1))} \right) \right] \right\} + F_\Lambda^{0+}(M) - e^{-M^2 S_E} F_\Lambda^{\tilde{S}_E(1)}(M). \quad (17)$$

Here, $\tilde{S}_E(x) = \tanh(xqBS_E)/qB$ and the auxiliary function is defined as

$$F_\Lambda^S(M) \equiv \int^\Lambda \frac{d^3 p}{2\pi^3} \int_{-\infty}^\infty \frac{dp_4}{2\pi} \frac{e^{-p_\perp^2 S}}{p_4^2 + E_p^2} = \int_0^\Lambda \frac{pdp}{\pi^2} \frac{D(pS^{1/2})}{S^{1/2} E_p} \quad (18)$$

with $p_\perp^2 = p_1^2 + p_2^2$, $E_p = \sqrt{\mathbf{p}^2 + M^2}$ and $D(x)$ the Dawson's integral function. In the large qB limit, $\tilde{S}_E(1) \rightarrow 0^+$ and $K^r(M, E, B)$ can be simply presented as the form $(1 - e^{-M^2 S_E}) \tilde{K}^r(M, E, B)$ with $\tilde{K}^r(M, E, B)$ the same as that in the IOF. Such a factorization is consistent with that given in Ref. [40]. The explicit forms of the "gap equations" in IIF can then be obtained by substituting Eqs. (14) and (15) into Eqs. (3) and (4), respectively. As long as the coupled "gap equations" can be solved self-consistently, the neutral pion condensate can be found to be simply

$$\pi^0 = \frac{qE q B}{4\pi^2} \left(1 - e^{-M^2 S_E}\right) \frac{2G}{m_0},$$

which is different from the one in IOF [37] by the extra term from Schwinger mechanism.

As we've already mentioned, there is no self-consistent thermodynamic potential for both the "gap equations" in IIF, because

$$\frac{\partial}{\partial \pi^0} \frac{1}{V_4} \text{Tr } \mathcal{S}(x, x) \neq \frac{\partial}{\partial m} \frac{1}{V_4} \text{Tr } \mathcal{S}(x, x) i\gamma^5$$

due to the SPP contributions in the last anomaly terms of Eqs.(14) and (15). This is not a big deal since the system is non-equilibrium *ab initio* in IIF and the thermodynamic potential or pressure might not be well defined. Nevertheless, there is a consistent thermodynamic potential for the anomaly irrelevant terms:

$$\Omega_{\text{IIF}} = \frac{(m - m_0)^2 + (\pi^0)^2}{4G} + N_c \Re \left\{ \int_0^\infty \frac{ds}{8\pi^2} \frac{e^{-M^2 s}}{s} \left[\frac{qB}{\tanh(qBs)} \frac{qE}{\tan(qEs)} - \frac{1}{s^2} - \frac{s e^{-M^2 S_E}}{s + S_E} \left(\frac{qB}{\tanh(qB(s + S_E))} \frac{qE}{\tan(qEs)} - \frac{1}{s(s + \tilde{S}_E(1))} \right) \right] - G_\Lambda^{0+}(M) + G_\Lambda^{\tilde{S}_E(1)}(M) \right\}, \quad (19)$$

where the auxiliary function is defined as

$$G_\Lambda^S(M) \equiv \int_0^M M' dM' e^{-M'^2 S_E} F_\Lambda^S(M') = \int_0^\Lambda \frac{pdp}{2\pi^{3/2}} \frac{e^{p^2 S_E} \left[\text{Erf} \left(S_E^{1/2} E_p \right) - \text{Erf} \left(S_E^{1/2} p \right) \right] D(pS^{1/2})}{S_E^{1/2} S^{1/2}} \quad (20)$$

with $\text{Erf}(x)$ the error function. We'd like to point out that: When chiral anomaly is not relevant to the ground state, such as in pure electric field and beyond the chiral rotation region in PEM, the quantity $-\Omega_{\text{IIF}} + \Omega_{\text{IIF}}|_{E, B \rightarrow 0}$ can

be roughly considered as the in-in pressure of the system. A part of the pressure is then from the persistent pair production.

In the end, it is useful to give the thermodynamic potential in IOF here, that is, $\Omega_{\text{IOF}} \equiv \bar{\Omega}_{\text{IOF}} + \Omega_{\text{a}}$ [45] with the anomaly term $\Omega_{\text{a}} = -N_c \frac{qEqB}{4\pi^2} \theta$ and the regular one

$$\bar{\Omega}_{\text{IOF}} = \frac{M^2 - 2Mm_0 \cos \theta + m_0^2}{4G} + N_c \Re \left\{ \int_0^\infty \frac{ds}{8\pi^2} \frac{e^{-M^2 s}}{s} \left[\frac{qB}{\tanh(qBs)} \frac{qE}{\tan(qEs)} - \frac{1}{s^2} \right] - G_\Lambda^{0+}(M) \right\}, \quad (21)$$

where the chiral condensates are presented alternatively in terms of the magnitude M and phase $\theta = \arcsin(\pi^0/M) = \arccos(m/M)$. Though the anomaly part Ω_{a} is a linear term of the angle variable θ , the 2π periodicity is automatically guaranteed for the physical results if we check the more fundamental quantity: the partition function of the system in real-time, that is

$$\mathcal{Z}_{\text{a}} = e^{-V_4 \Omega_{\text{a}}} = e^{iQ\theta}, \quad Q = \left[VN_c \frac{qEqB}{4\pi^2} \right]. \quad (22)$$

Here, we defined the winding number $Q \in \mathbb{N}^+$ for $qEqB > 0$ by following the spirit of chiral anomaly [46] and the symbol $[x]$ denotes natural number equal to or smaller than positive x . For large Q as expected if the time-space volume V is very large, the approximation $Q \approx VN_c \frac{qEqB}{4\pi^2}$ can be used as long as we constrain ourselves to one period regime of θ by applying $\text{mod}(\theta, 2\pi)$.

However, the preferred value of θ depends on the regime we choose for $\text{mod}(\theta, 2\pi)$ and is a boundary minimum, which means not any value is really preferred at all and the phase can change randomly. For later convenience, we get rid of the mod function here as long as no physical ambiguity is induced.

III. POLARIZATION FUNCTIONS IN REAL-TIME FORMALISM

As the lengthy derivations of the polarization functions for the neutral sector were already given in Ref. [38] for IOF, we present the corresponding derivations and regularizations for IIF in this section. Adopting the effective quark propagator in Eq.(13), the polarization function of $\hat{\pi}^0$ boson with only energy q_0 nonzero can be evaluated as the following:

$$\begin{aligned} \Pi_{\hat{\pi}^0 \hat{\pi}^0}(B, E, q_0) &\equiv -i \int \frac{d^4 p}{(2\pi)^4} \text{Tr} \hat{S}(p + q_0) i\gamma_5 \hat{S}(p) i\gamma_5 \\ &= N_c \frac{qEqB}{4\pi^2} \int_{\Gamma_\epsilon} ds \int_{\Gamma_\epsilon} ds' \exp \left\{ -i \left[(M^2 - i\eta) s_+ - \frac{\tanh(qEs) \tanh(qEs')}{qE(\tanh(qEs) + \tanh(qEs'))} q_0^2 \right] \right\} \left\{ -2m\pi^0 + \right. \\ &\quad \left. \frac{(\pi^0)^2 - m^2}{\tanh(qEs_+) \tan(qBs_+)} + \frac{iqB \sin^{-2}(qBs_+)}{\tanh(qEs_+)} + \frac{iqE \sinh^{-2}(qEs_+)}{\tan(qBs_+)} - \frac{q_0^2 \tanh(qEs) \tanh(qEs') \sinh^{-2}(qEs_+)}{(\tanh(qEs) + \tanh(qEs')) \tan(qBs_+)} \right\} \\ &= \frac{N_c}{8\pi^2} \int_0^\infty t dt \int_{-1}^1 du \exp \left\{ -i \left[(M^2 - i\eta) t - \frac{\tanh(qEt^+) \tanh(qEt^-)}{qE(\tanh(qEt^+) + \tanh(qEt^-))} q_0^2 \right] \right\} \sum_{x=0}^2 \bar{\Pi}_{\hat{\pi}^0 \hat{\pi}^0}^x(E, B, q_0), \quad (23) \end{aligned}$$

where $s_\pm = s \pm s'$, $t^\pm = \frac{t(1 \pm u)}{2}$ and the auxiliary functions in the integrand are defined as

$$\begin{aligned} &\bar{\Pi}_{\hat{\pi}^0 \hat{\pi}^0}^0(E, B, q_0)/(qEqB) \\ &= \left\{ -2m\pi^0 - \frac{q_0^2 \tanh(qEt^+) \tanh(qEt^-) \sinh^{-2}(qEt)}{(\tanh(qEt^+) + \tanh(qEt^-)) \tan(qBt)} + \frac{1}{\tanh(qEt) \tan(qBt)} \left[\frac{i}{t} + 2(\pi^0)^2 \right. \right. \\ &\quad \left. \left. + \frac{q_0^2}{2} \text{csch}(qEt) \left(u \sinh(qEtu) - \coth(qEt) \cosh(qEtu) + \text{csch}(qEt) \right) \right] \right\}, \quad (24) \end{aligned}$$

$$\begin{aligned} &\bar{\Pi}_{\hat{\pi}^0 \hat{\pi}^0}^x(E, B, q_0)/(qEqB) \\ &= f(x) e^{-xM^2 S_E} \left\{ -2m\pi^0 + \frac{(\pi^0)^2 - m^2}{\tanh(qEt) \tan(qB(t - ixS_E))} + \frac{iqB \sin^{-2}(qB(t - ixS_E))}{\tanh(qEt)} + \frac{iqE \sinh^{-2}(qEt)}{\tan(qB(t - ixS_E))} \right. \\ &\quad \left. - \frac{q_0^2 \tanh(qEt^+) \tanh(qEt^-) \sinh^{-2}(qEt)}{(\tanh(qEt^+) + \tanh(qEt^-)) \tan(qB(t - ixS_E))} \right\}, \quad x = 1, 2 \quad (25) \end{aligned}$$

with $f(x) = 3x^2 - 6x + 1$. In the last step of Eq.(23), we've used partial integral to remove the seemed divergent term $\sim \sin^{-2}(qBt)$ in $\bar{\Pi}_{\hat{\pi}^0\hat{\pi}^0}^0$ according to the non-overlapping condition [47], which implies that the higher order divergence at $t = 0$ is nonphysical and can be reduced to $\sim \cot(qBt)$ through partial integral. Besides, the divergence at $t = n\pi$ ($n \in \mathbb{N}_+$) is an artifact that is introduced when we stick to the integration path of t along real axis by taking its infinitesimal negative imaginary component [40] to zero. The application of non-overlapping condition avoids the artifact automatically when Cauchy principal value integration is kept in mind.

Then, $\bar{\Pi}_{\hat{\pi}^0\hat{\pi}^0}^0$ can be regularized in the same way as that in Ref. [38]. For the terms with $x = 1, 2$, the integrations can be regularized in the "subtraction-addition" scheme, that has been utilized for the gap equations, as

$$\begin{aligned} & \Pi_{\hat{\pi}^0\hat{\pi}^0}^{x r}(B, E, q_0) \\ &= \frac{N_c}{8\pi^2} \int_0^\infty t dt \int_{-1}^1 du \left(\exp \left\{ -i \left[(M^2 - i\eta)t - \frac{\tanh(qEt^+) \tanh(qEt^-)}{qE(\tanh(qEt^+) + \tanh(qEt^-))} q_0^2 \right] \right\} \right) \bar{\Pi}_{\hat{\pi}^0\hat{\pi}^0}^x(E, B, q_0) \\ & \quad - f(x) e^{-xM^2 S_E} e^{-it \left[(M^2 - i\eta) - \frac{1-u^2}{4} q_0^2 \right]} \left\{ \frac{(\pi^0)^2 - m^2}{t(t - i\tilde{S}_E(x))} + \frac{i}{t(t - i\tilde{S}_E(x))^2} + \frac{i}{t^2(t - i\tilde{S}_E(x))} - \frac{q_0^2 \frac{(1-u^2)}{4}}{t(t - i\tilde{S}_E(x))} \right\} \\ & \quad + \Pi_{\hat{\pi}^0\hat{\pi}^0}^{x \Lambda}(E, B, q_0). \end{aligned} \quad (26)$$

Altogether, the regularized polarization function for $\hat{\pi}^0$ meson is just

$$\Pi_{\hat{\pi}^0\hat{\pi}^0}^r(B, E, q_0) = \sum_{x=0}^2 \Pi_{\hat{\pi}^0\hat{\pi}^0}^{x r}(B, E, q_0),$$

and the regularized $\hat{\sigma}$ - and mixing-mode polarization functions can be given similarly as the following:

$$\begin{aligned} & \Pi_{\hat{\sigma}\hat{\sigma}}^r(B, E, q_0) \equiv \text{Reg} \left[-i \int \frac{d^4 p}{(2\pi)^4} \text{Tr} \hat{S}(p + q_0) \hat{S}(p) \right] = \Pi_{\hat{\pi}^0\hat{\pi}^0}^r(B, E, q_0) \Big|_{m \rightarrow -\pi^0}, \quad (27) \\ & \Pi_{\hat{\sigma}\hat{\pi}^0}^r(B, E, q_0) = \Pi_{\hat{\pi}^0\hat{\sigma}}^r(B, E, q_0) \equiv \text{Reg} \left[-i \int \frac{d^4 p}{(2\pi)^4} \text{Tr} \hat{S}(p + q_0) i\gamma_5 \hat{S}(p) \right] \\ &= \frac{N_c}{8\pi^2} \int_0^\infty t dt \int_{-1}^1 du \sum_{x=0}^2 f(x) e^{-xM^2 S_E} \left(\exp \left\{ -i \left[(M^2 - i\eta)t - \frac{\tanh(qEt^+) \tanh(qEt^-)}{qE(\tanh(qEt^+) + \tanh(qEt^-))} q_0^2 \right] \right\} \right) \left[qE qB \right. \\ & \quad \left. (m^2 - (\pi^0)^2) + \frac{2qE qB m\pi^0}{\tan(qB(t - i x S_E)) \tanh(qEt)} - e^{-it \left[(M^2 - i\eta) - \frac{1-u^2}{4} q_0^2 \right]} \frac{2m\pi^0}{t(t - i\tilde{S}_E(x))} \right] + \sum_{x=0}^2 \Pi_{\hat{\sigma}\hat{\pi}^0}^{x \Lambda}(E, B, q_0) \quad (28) \end{aligned}$$

Finally, the "addition" terms can be evaluated alternatively within the three-momentum cutoff scheme [38] as:

$$\begin{aligned} & \Pi_{\hat{\pi}^0\hat{\pi}^0}^{x \Lambda}(E, B, q_0) \\ &= \frac{N_c}{4\pi^2} f(x) e^{-xM^2 S_E} \int_0^\infty ds \int_0^\infty ds' \frac{e^{-i \left[(M^2 - i\eta) s_+ - \frac{ss'}{s_+} q_0^2 \right]}}{s_+(s_+ - i\tilde{S}_E(x))} \left[(\pi^0)^2 - m^2 + \frac{i}{s_+ - i\tilde{S}_E(x)} + \frac{i}{s_+} - q_0^2 \frac{ss'}{s_+^2} \right] \\ &= i \frac{N_c}{4\pi^4} f(x) \int d^4 p e^{-xM^2 S_E - \tilde{S}_E(x) p_\perp^2} \int_0^\infty ds \int_0^\infty ds' e^{-i \left[(E_p^2 - i\eta) s_+ - s' p_0^2 - s(p_0 + q_0)^2 \right]} \left[(\pi^0)^2 - m^2 - \mathbf{p}^2 + (p_0 + q_0) p_0 \right] \\ &= -i \frac{N_c}{4\pi^4} f(x) \int d^4 p e^{-xM^2 S_E - \tilde{S}_E(x) p_\perp^2} \frac{(\pi^0)^2 - m^2 - \mathbf{p}^2 + (p_0 + q_0) p_0}{[(p_0 + q_0)^2 - E_p^2][p_0^2 - E_p^2]} = \frac{N_c}{\pi^3} f(x) \int d^3 \mathbf{p} e^{-xM^2 S_E - \tilde{S}_E(x) p_\perp^2} \frac{m^2 + \mathbf{p}^2}{E_p(q_0^2 - 4E_p^2)} \\ &= \frac{4N_c}{\pi^2} f(x) e^{-xM^2 S_E} \int_0^\Lambda p^2 dp \frac{D(\tilde{S}_E^{1/2}(x)p)}{\tilde{S}_E^{1/2}(x)p} \frac{m^2 + p^2}{E_p(q_0^2 - 4E_p^2)}, \quad (29) \end{aligned}$$

$$\begin{aligned}
& \Pi_{\tilde{\sigma}\tilde{\pi}^0}^x \Lambda(E, B, q_0) \\
&= m\pi^0 \frac{N_c}{2\pi^2} f(x) e^{-xM^2 S_E} \int_0^\infty ds \int_0^\infty ds' \frac{e^{-i[(M^2-i\eta)s_+ - \frac{ss'}{s_+} q_0^2]}}{s_+(s_+ - i\tilde{S}_E(x))} \\
&= i m\pi^0 \frac{N_c}{2\pi^4} f(x) \int d^4 p e^{-xM^2 S_E - \tilde{S}_E(x) p_\perp^2} \int_0^\infty ds \int_0^\infty ds' e^{-i[(E_p^2 - i\eta)s_+ - s' p_0^2 - s(p_0 + q_0)^2]} \\
&= -i \frac{N_c}{2\pi^4} f(x) \int d^4 p e^{-xM^2 S_E - \tilde{S}_E(x) p_\perp^2} \frac{m\pi^0}{[(p_0 + q_0)^2 - E_p^2][p_0^2 - E_p^2]} = -\frac{N_c}{\pi^3} f(x) \int d^3 \mathbf{p} e^{-xM^2 S_E - \tilde{S}_E(x) p_\perp^2} \frac{m\pi^0}{E_p(q_0^2 - 4E_p^2)} \\
&= -\frac{4N_c}{\pi^2} f(x) e^{-xM^2 S_E} \int_0^\Lambda p^2 dp \frac{D(\tilde{S}_E^{1/2}(x)p)}{\tilde{S}_E^{1/2}(x)p} \frac{m\pi^0}{E_p(q_0^2 - 4E_p^2)}, \tag{30}
\end{aligned}$$

which are consistent with the regularized vacuum terms $\Pi_{\tilde{\pi}^0\tilde{\pi}^0}^\Lambda$ and $\Pi_{\tilde{\sigma}\tilde{\pi}^0}^\Lambda$ in Ref. [38] if we set $x = 0$.

IV. NUMERICAL CALCULATIONS

In order to perform numerical calculations and compare to QCD, the three parameters of the NJL model are fixed to $G = 9.86 \text{ GeV}^{-2}$, $\Lambda = 0.653 \text{ GeV}$ and $m_0 = 5 \text{ MeV}$ by fitting the neutral pion mass $m_\pi = 134 \text{ MeV}$, pion decay constant $f_\pi = 93 \text{ MeV}$ and chiral condensate $\langle \bar{\psi}\psi \rangle = -(0.25 \text{ GeV})^3$ physically [25]. For the purpose of improving the convergence of the proper-time integrals, especially those involved in the polarization functions, the variable s can be rotated by an angle to $\frac{1-C_s i}{\sqrt{1+C_s^2}} s$ ($C_s \geq 0$) in the complex plane. We've checked carefully that the numerical results do not depend on the value of C_s as no singularity is ever encountered during the rotation, so we simply set $C_s = 1$ in the calculations. Another trick that can be adopted for the sake of convergence, especially when $q_0 \gtrsim 2M$, is that the subtract terms in Eqs. (26) and (28) can be approximated by the ones with small enough EM field while keeping S_E and $\tilde{S}_E(x)$ fixed. Take the simplest term in $\Pi_{\tilde{\sigma}\tilde{\pi}^0}^r$ for example, we can take the following approximation:

$$\begin{aligned}
& \frac{2m\pi^0 e^{-it[(M^2-i\eta) - \frac{1-u^2}{4} q_0^2]}}{t(t - i\tilde{S}_E(x))} \\
& \approx \frac{2qE_0 m\pi^0 e^{-i[(M^2-i\eta)t - \frac{\tanh(qE_0 t^+) \tanh(qE_0 t^-) q_0^2}{qE_0(\tanh(qE_0 t^+) + \tanh(qE_0 t^-))}]}{\tanh(qE_0 t)(t - i\tilde{S}_E(x))}
\end{aligned}$$

with $eE_0 = 10^{-3} \text{ GeV}^2$.

A. Pure electric field

As a warm-up, we first consider the much simpler pure electric field limit with $B \rightarrow 0$, thus no chiral anomaly is induced by the background EM field and the pseudoscalar condensate $\pi^0 = 0$ [48]. Illuminated in the upper and lower panels of Fig. 1 are the evolutions of the order parameter m for chiral symmetry and the pole mass m_π of the Goldstone-like mode $\tilde{\pi}^0$ with electric field eE , respectively. Similar features are found in the IOF and IIF: With m continuously decreasing with eE , the pion mass

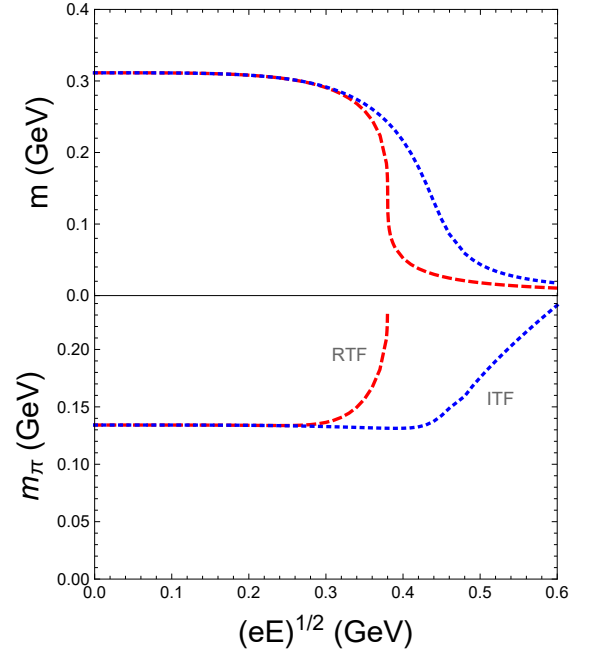


FIG. 1. The dynamical quark mass m and neutral pion mass m_π as functions of external electric field eE in the IOF (blue dotted lines) and IIF (red dashed lines), respectively.

m_π decreases (though slightly) and then increases across the transition region, which is pretty like the crossover feature at finite temperature [25, 26]. However, compared to the results in the IOF, we find that the feedback of SPP becomes prominent around the point $qE \sim m^2$ in the IIF, which then further catalyzes chiral symmetry restoration due to the medium effect. As a consequence, the variations of m and m_π become much stiffer around the transition region – actually, in chiral limit, the chiral symmetry restoration is of second-order in the IOF but of first-order in the IIF.

B. Parallel electromagnetic field

In the parallel electromagnetic field with $B = E$, the comparisons between the chiral condensates in the IOF and IIF are illuminated in Fig. 2: The evolutions of m are almost the same up to the end of chiral rotation thus are denoted by a single black solid line. As we can see, the value of π^0 diverges beyond the point $(qE)^{1/2} \geq \pi^0$ where the SPP starts to play an important role. As demonstrated clearly by the feature of m , our recent more careful check indicates that the phase transition is not of second-order [37, 38] but rather of very weak first-order at the end of chiral rotation with $(eE_{c1})^{1/2} = 0.217$ GeV. Surprisingly, the chiral restoration becomes of first-order in the IIF rather than second-order in the IOF (see the curves of π^0). Nevertheless, this is qualitatively consistent with the stiffer feature found in the previous case with pure electric field and the fact that the Schwinger mechanism is enhanced due to the presence of parallel magnetic field [39].

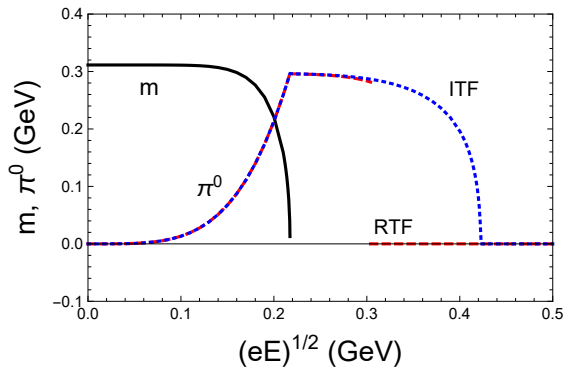


FIG. 2. The illuminations of π^0 as a function of electric field eE in the IOF (blue dotted lines) and IIF (red dashed lines), respectively. The evolutions of m are almost the same up to the end of chiral rotation thus are denoted by a single black solid line.

Accordingly, the mass eigenstates of the collective modes: the Goldstone-like Π^0 and the Higgs-like Σ are studied and their pole masses are illuminated together with the parity mixing angles in Figs. 3 and 4, respectively. Compared to our previous explorations [38], the recent more precise calculations find nonmonotonic features of both Π^0 and Σ masses with EM field. However, the mixing angles both monotonically decrease from 0 to $\sim -\pi/2$, which indicates the role exchange between the parity eigenstates $\hat{\pi}^0$ and $\hat{\sigma}$, consistent with the condensate exchange during the chiral rotation as shown in Fig.2.

One terrible thing happens around the end point of chiral rotation: the Π^0 mass decreases to zero, which may imply the instability of the ground state with only π^0 condensation by following Ginzburg-Landau theory. We plot the θ dependence of the thermodynamic potential $\Delta\Omega_\theta = \Omega_\theta - \Omega_0$ for chosen EM fields in Fig. 5. In the vacuum without EM field, there are infinite degenerate

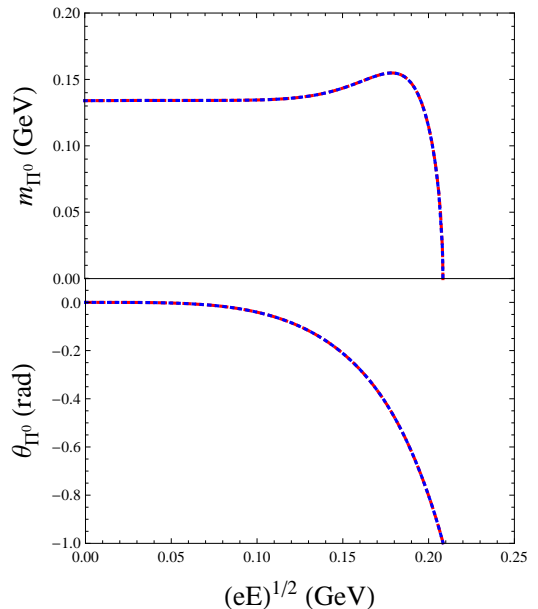


FIG. 3. The mass m_{Π^0} of the Goldstone-like collective mode and the corresponding parity mixing angle θ_{Π^0} as functions of electric field eE in the IOF (blue dotted lines) and IIF (red dashed lines), respectively. $\theta_{\Pi^0} = 0$ corresponds to the normal pseudoscalar meson π^0 .

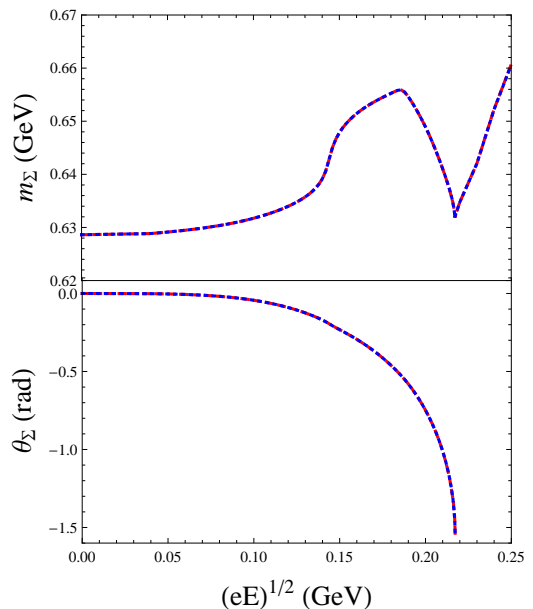


FIG. 4. The mass m_Σ of the Higgs-like collective mode and the corresponding parity mixing angle θ_Σ as functions of electric field eE in the IOF (blue dotted lines) and IIF (red dashed lines), respectively. $\theta_\Sigma = 0$ corresponds to the normal scalar meson σ .

global minima locating at $\theta = 2k\pi$ ($k \in \mathbb{Z}$), which is con-

sistent with σ condensation found before [25, 26]. With increasing EM field, the global minima become local ones locating at $\theta = \theta_{EM} + 2k\pi$ with $\theta_{EM} \in (-\pi, \pi)$ EM-dependent and π^0 condensate also forms. Eventually, at the critical point eE_{c1} , the local minima disappear and $\Delta\Omega_\theta$ becomes a monotonic function of θ , just like the term induced by chiral anomaly: $\Delta\Omega_\theta = -N_c \frac{qEgB}{4\pi^2} \theta$ in free Fermi gas system with finite fermion mass and electric charge. In the free case, a simple functional variable transformation $\psi \rightarrow e^{-i\gamma^5 \theta} \psi$ will give rise to such a term, which then forces the chiral angle θ to change all the time as there is no minimum. This is the source of instability encountered at eE_{c1} : As the expectation value of the chiral phase θ keeps changing, the phase fluctuation Π^0 is never a well-defined collective mode. Keep in mind that this is different from the case without EM field and in chiral limit, where the thermodynamic potential Ω is θ -independent and the massless phase excitation mode itself shifts the expectation value of θ randomly.

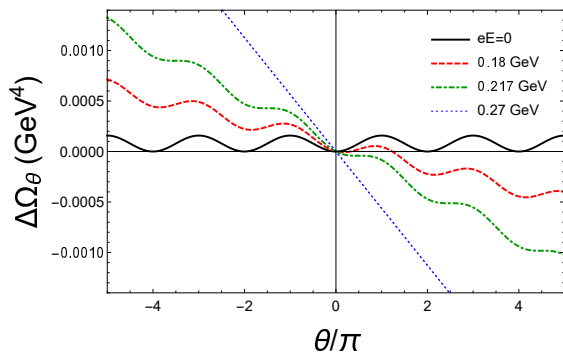


FIG. 5. The θ dependence of the thermodynamic potential $\Delta\Omega_\theta = \Omega_\theta - \Omega_0$ for chosen electric fields $eE = 0, 0.18, 0.217$ and 0.27 GeV. The blue dotted line corresponds to the free case with $\Delta\Omega_\theta = -N_c \frac{qEgB}{4\pi^2} \theta$.

For the Higgs-like mode, there is no such problem because it corresponds to the magnitude of the "order parameter" of chiral symmetry. As θ keeps changing, the curves of π^0 condensate beyond the critical point eE_{c1} in Fig. 2 should be understood as those of the magnitude M . Along with the chiral restoration in PEM field, the magnitude excitation mode Σ can be studied even beyond eE_{c1} : The pole mass of Σ starts to increase with EM field, see Fig. 4. Thus, even though the chiral restoration

feature of M up to $(eE)^{1/2} = 0.25$ GeV is quite similar to that at finite temperature, the response of Σ mode is rather different. In the previous study, it was found that [26]: with temperature increasing up to the pseudo-critical point, the pole mass of σ meson decreases down to a value close to that of pion mesons. We've checked that the qualitative difference is not due to the mixing term $\Pi_{\sigma\pi^0}^r$ induced by PEM field, so the cause might just be the interplay between electric and magnetic field effects; refer to Ref. [45] for more discussions on the interplay.

V. SUMMARY

In this work, we compare the effects of electromagnetic fields on strong coupling systems within in-out and in-in formalisms under the framework of one-flavor Nambu–Jona-Lasinio model. The main physical difference between the IOF and IIF is that the feedback of Schwinger pair production is also taken into account in the later. In the pure electric field case, we find that the SPP effect further catalyzes chiral symmetry restoration beyond the pair instable point $qE \sim m^2$. This feature remains in parallel EM field, but the effect on chiral rotation is negligible because only small EM field is relevant at this stage. We study the chiral rotation and the corresponding mass eigen collective modes with more precision than that in Ref. [38] and find: the transition is of weak first-order rather than of second-order [37] at the end of chiral rotation eE_{c1} and the masses of both the Goldstone-like and Higgs-like modes show nonmonotonic behaviors there.

At the chiral rotation stage, one serious problem is that the mass of the Goldstone-like mode Π^0 decreases to zero around eE_{c1} , which seems to indicate a "wrong" ground state we've proposed. This instability is actually related to the chiral anomaly induced by PEM field and corresponds to a "chaotic" state for the chiral phase, similar to that in free Fermi gas system with finite fermion mass and electric charge. After clarifying the instability, we're now at a point ready to extend the research on PEM effect to the realistic three-flavor case, where more pseudoscalar condensations and parity mixing are involved.

Acknowledgments— G.C. thanks X.-G. Huang and L. Wang for their comments on this work. G.C. is supported by the National Natural Science Foundation of China with Grant No. 11805290 and Young Teachers Training Program of Sun Yat-Sen University with Grant No. 19lgpy282.

[1] V. Skokov, A. Y. Illarionov and V. Toneev, Int. J. Mod. Phys. A **24**, 5925 (2009).
 [2] W. T. Deng and X. G. Huang, Phys. Rev. C **85**, 044907 (2012).
 [3] W. T. Deng and X. G. Huang, Phys. Lett. B **742**, 296 (2015).
 [4] J. Błoczynski, X. G. Huang, X. Zhang and J. Liao, Phys. Lett. B **718**, 1529 (2013).
 [5] V. P. Gusynin, V. A. Miransky and I. A. Shovkovy, Phys.

Rev. Lett. **73**, 3499 (1994) Erratum: [Phys. Rev. Lett. **76**, 1005 (1996)].
 [6] V. P. Gusynin, V. A. Miransky and I. A. Shovkovy, Phys. Lett. B **349**, 477 (1995).
 [7] G. S. Bali, F. Bruckmann, G. Endrodi, Z. Fodor, S. D. Katz, S. Krieg, A. Schafer and K. K. Szabo, JHEP **1202**, 044 (2012).
 [8] G. S. Bali, F. Bruckmann, G. Endrodi, Z. Fodor, S. D. Katz and A. Schafer, Phys. Rev. D **86**, 071502

- (2012).
- [9] F. Bruckmann, G. Endrodi and T. G. Kovacs, *JHEP* **1304**, 112 (2013).
- [10] K. Fukushima and Y. Hidaka, *Phys. Rev. Lett.* **110**, no. 3, 031601 (2013).
- [11] T. Kojo and N. Su, *Phys. Lett. B* **720**, 192 (2013).
- [12] K. Hattori, T. Kojo and N. Su, *Nucl. Phys. A* **951** (2016) 1.
- [13] J. Chao, P. Chu and M. Huang, *Phys. Rev. D* **88**, 054009 (2013).
- [14] G. Cao, L. He and P. Zhuang, *Phys. Rev. D* **90**, no. 5, 056005 (2014).
- [15] E. J. Ferrer, V. de la Incera and X. J. Wen, *Phys. Rev. D* **91**, no. 5, 054006 (2015).
- [16] S. Mao, *Phys. Lett. B* **758**, 195 (2016).
- [17] Y. Hidaka and A. Yamamoto, *Phys. Rev. D* **87**, no. 9, 094502 (2013).
- [18] G. S. Bali, B. B. Brandt, G. Endrodi and B. Glassle, *Phys. Rev. D* **97**, no. 3, 034505 (2018).
- [19] S. S. Avancini, R. L. S. Farias, M. Benghi Pinto, W. R. Tavares and V. S. Timteo, *Phys. Lett. B* **767**, 247 (2017).
- [20] Z. Wang and P. Zhuang, *Phys. Rev. D* **97**, no. 3, 034026 (2018).
- [21] S. Mao, *Phys. Rev. D* **99**, no. 5, 056005 (2019).
- [22] H. Liu, X. Wang, L. Yu and M. Huang, *Phys. Rev. D* **97**, no. 7, 076008 (2018).
- [23] M. Coppola, D. Gmez Dumm and N. N. Scoccola, *Phys. Lett. B* **782**, 155 (2018).
- [24] G. Cao, *Phys. Rev. D* **100**, no. 7, 074024 (2019).
- [25] P. Zhuang, J. Hufner and S. P. Klevansky, *Nucl. Phys. A* **576**, 525 (1994).
- [26] S. P. Klevansky and R. H. Lemmer, *Phys. Rev. D* **39**, 3478 (1989).
- [27] D. E. Kharzeev, L. D. McLerran and H. J. Warringa, *Nucl. Phys. A* **803**, 227 (2008).
- [28] K. Fukushima, D. E. Kharzeev and H. J. Warringa, *Phys. Rev. D* **78**, 074033 (2008).
- [29] D. E. Kharzeev and H. U. Yee, *Phys. Rev. D* **83**, 085007 (2011).
- [30] D. T. Son and A. R. Zhitnitsky, *Phys. Rev. D* **70**, 074018 (2004).
- [31] M. A. Metlitski and A. R. Zhitnitsky, *Phys. Rev. D* **72**, 045011 (2005).
- [32] X. G. Huang and J. Liao, *Phys. Rev. Lett.* **110**, no. 23, 232302 (2013).
- [33] K. Hattori and Y. Yin, *Phys. Rev. Lett.* **117**, no. 15, 152002 (2016).
- [34] J. Liao, *Pramana* **84**, no. 5, 901 (2015).
- [35] D. E. Kharzeev, J. Liao, S. A. Voloshin and G. Wang, *Prog. Part. Nucl. Phys.* **88**, 1 (2016).
- [36] X. G. Huang, *Rept. Prog. Phys.* **79**, no. 7, 076302 (2016).
- [37] G. Cao and X. G. Huang, *Phys. Lett. B* **757**, 1 (2016).
- [38] L. Wang, G. Cao, X. G. Huang and P. Zhuang, *Phys. Lett. B* **780**, 273 (2018).
- [39] P. Copinger and K. Fukushima, *Phys. Rev. Lett.* **117**, no. 8, 081603 (2016) Erratum: [*Phys. Rev. Lett.* **118**, no. 9, 099903 (2017)].
- [40] P. Copinger, K. Fukushima and S. Pu, *Phys. Rev. Lett.* **121**, no. 26, 261602 (2018).
- [41] T. D. Cohen and D. A. McGady, *Phys. Rev. D* **78**, 036008 (2008).
- [42] E. Fradkin, D. Guitman, and S. Shvartsman, *Quantum Electrodynamics: With Unstable Vacuum*, Springer Series in Nuclear and Particle Physics (Springer-Verlag, Berlin, 1991).
- [43] Y. Nambu and G. Jona-Lasinio, *Phys. Rev.* **124**, 246 (1961).
- [44] Y. Nambu and G. Jona-Lasinio, *Phys. Rev.* **122**, 345 (1961).
- [45] L. Wang and G. Cao, *Phys. Rev. D* **97**, no. 3, 034014 (2018).
- [46] S. Weinberg, *The Quantum Theory of Fields: Modern Applications*, (Cambridge University Press, Cambridge, 1996) Vol. II, Chap. 23, P455-462.
- [47] J. Schwinger, *Particles, Sources and Fields* (Addison-Wesley, Reading, Mass. , 1973), Vol. II, Chap. 4,- Secs. 14-16.
- [48] G. Cao and X. G. Huang, *Phys. Rev. D* **93**, no. 1, 016007 (2016).